SIMULATION OF THE EFFECT OF CORRUGATED STRUCTURES ON THE LONGITUDINAL BEAM DYNAMICS AT KARA

S. Maier*, M. Brosi†, A. Mochihashi, M. J. Nasse, P. Schreiber, M. Schwarz,
A.-S. Müller, Karlsruhe Institute of Technology, Karlsruhe, Germany

Abstract

Two parallel corrugated plates will be installed at the KIT storage ring KARA (KArlsruhe Research Accelerator). This impedance manipulation structure will be used to study and eventually control the beam dynamics and the emitted coherent synchrotron radiation (CSR). In this contribution, we present the influence of the parameters of the structure on its impedance and the results obtained with the Vlasov-Fokker-Planck solver Inovesa showing the impedance impact of different corrugated structures on the CSR power.

INTRODUCTION

In contrast to incoherent radiation, CSR scales quadratically with the number of particles and therefore enhances the photon flux by several orders of magnitudes. As the emission is coherent for wavelengths larger than the bunch length, high electron density and short bunches are necessary to extend CSR to higher frequencies and to increase the intensity of the radiation. In such short bunch regimes complex nonlinear phenomena can occur due to the interaction between the passing bunch and its emitted CSR. This results in dynamic instabilities and bunch deformations like the so-called microbunching instability [1]. This instability can cause longitudinal substructures on the bunches generating intense THz radiation.

At KIT, we are developing and designing a versatile impedance chamber for the KARA storage ring to study the microbunching instability by manipulating the wakefield and thereby affecting the longitudinal beam dynamics of the electrons. The additional impedance and the resulting wakefield change will be generated by two horizontal parallel plates with periodic rectangular corrugations. Although Bane *et al.* [2, 3] showed that narrow-band THz pulses can be generated by installing such structure into a linear accelerator, to our knowledge such a structure has never been installed into a storage ring, where the electrons pass the structure multiple times. In Fig. 1, a schematic drawing with the characteristic parameters periodic length L, corrugation depth h and corrugation width g, as well as the plate distance $2b$ is given. The theoretical longitudinal impedance $Z^{\parallel}$ for parallel corrugated plates is given by Ng *et al.* [4] under the assumptions $L \lesssim h \ll b$ as

$$\frac{Z^{\parallel}}{L} = \frac{Z_{\text{vac.}}}{\pi b^2} \left[\pi k_{\text{res}} \delta \left(k^2 - k_{\text{res}}^2 \right) + i \cdot \text{P.V.} \left(\frac{k}{k^2 - k_{\text{res}}^2} \right) \right] \tag{1}$$

with the resonance wave number $k_{\text{res}} = \sqrt{\frac{2L}{bgh}}$, wave number

---

* sebastian.maier@kit.edu
† Now at MAX IV Laboratory, Lund, Sweden
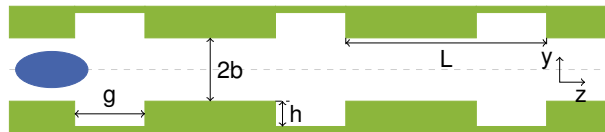
Figure 1: The corrugated plates in cross section with the relevant geometric parameters are shown. The electron bunch is indicated in blue.

$k = \frac{\omega}{c}$, the vacuum impedance $Z_{\text{vac.}}$, the δ-distribution, and principal value P.V.(x).

Previous impedance simulations with CST Studio [5] have shown how the parameters of the structure influence the impedance and that the results are in good agreement with the theoretical prediction [6]. The impedance can be described by the resonator model [7], which is characterized by the three parameters resonance frequency f_{res}, the shunt impedance Z_0, and the quality factor Q.

The resonance frequency of the investigated impedance is in the range between 50 GHz and 200 GHz, where a fraction of the CSR impedance is shielded by the beam pipe and therefore an additional impedance with Z_0=1 kΩ has a significant contribution to the total impedance of the KARA storage ring.

SIMULATION

For the beam dynamics simulations Inovesa [8], an in-house developed Vlasov-Fokker-Planck solver, is used, which describes the micro-bunching instability at the KARA storage ring [9] very well. For the results presented in this contribution, the settings were chosen so that they are comparable to the KARA short-bunch operation mode with synchrotron frequency $f_{\text{sync}} = 9.44$ kHz and the acceleration voltage $V_{\text{RF}} = 1.048$ MV at a beam energy of $E = 1.3$ GeV.

For modeling the storage ring impedance the dominating CSR parallel plate impedance is used [10], which already has proven to govern the microbunching instability [9,11] for KARA. The additional impedance of the corrugated plates is modelled by the resonator model with its parameters f_{res}, Z_0, Q. The impedance simulation for the corrugated structure has shown [6], that a quality factor $Q = 3$ and a shunt impedance $Z_0 = 1$ kΩ are suitable for a structure length of 20 cm, which is the maximum space available along the beampipe in KARA. As long as it is not explicitly mentioned, these values are used for the Inovesa simulations.

Above the threshold current I_{thr} of the microbunching instability the first fluctuations of the CSR intensity occur. Therefore, the behaviour of the standard deviation (STD) of the CSR emission as function of the bunch current indicates
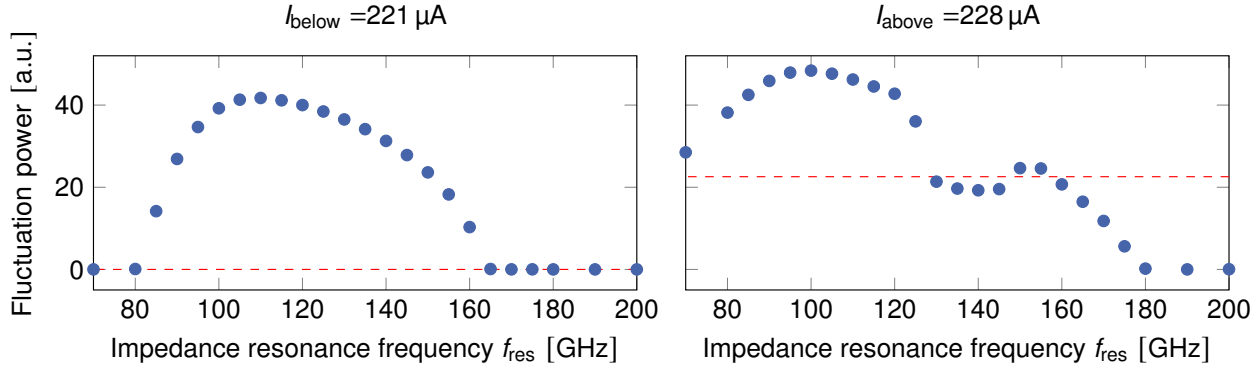
Figure 2: Fluctuation power at the bursting frequency f_{burst} for additional corrugation impedances with different resonance frequencies f_{res} and fixed shunt impedance $Z_0 = 1\,k\Omega$ and quality factor $Q = 3$ at a beam current below (left) and above (right) the unperturbed bursting threshold. The red dashed line indicates the intensity without the additional impedance.

the threshold current, because it increases drastically above the instability threshold, so a kink at the threshold current is visible [12]. However, certain additional impedances change the beam dynamics in such a way, that the bursting threshold cannot be determined properly by this method. Alternatively, since the fluctuation power at the bursting frequency - the main frequency in the intensity fluctuations of the CSR during the microbunching instability - is drastically reduced in amplitude below the threshold current, this parameter, which is closely related to the STD of the CSR intensity, can be used to determine the threshold current. For the case considered here both methods come to the same results for the threshold current ($I_{thr} = 226\,\mu A$) and the bursting frequency at the threshold ($f_{burst} = 34.6\,kHz$) for the simulation setting without additional impedance.

IMPEDANCE SCAN

For the design of the corrugated structure it is of great interest how the microbunching instability is affected by an additional impedance. For this purpose two currents, one slightly above ($I_{above} = 228\,\mu A$) and one below ($I_{below} = 221\,\mu A$) the unperturbed threshold current, have been chosen to simulate the beam dynamics and the temporal development of the emitted radiation intensity for different additional corrugation impedances with varying resonance frequencies. The Fourier transform of the simulated emitted CSR shows the fluctuation frequency of the radiation and therefore points out the dominant frequencies of the microbunching. In Fig. 2, the fluctuation power at the bursting frequency corresponding to the maximum intensity is displayed as a function of the additional impedance resonance frequency for the two above-mentioned currents.

For $I_{below} = 221\,\mu A$, i.e., below the unperturbed threshold current, there is no significant emitted CSR power without an additional impedance (red dashed line). However, certain impedances lead to a high power fluctuation that is comparable to or even higher than the fluctuation power directly above the unperturbed threshold but without an additional

impedance. This is the case for an impedance resonance frequency in a range from 85 GHz to 160 GHz. Here, the bursting threshold is reduced to a value below I_{below}, causing the instability to still occur at I_{below}. In contrast, a higher or smaller resonance frequency does not seem to affect the emitted CSR power and therefore does not reduce the threshold current below I_{below}. For $I_{above} = 228\,\mu A$, i.e., above the unperturbed threshold current, the fluctuation power is amplified for $f_{res} < 130\,GHz$, where the maximum increase is at about $f_{res} = 100\,GHz$ and results in more than doubling of the fluctuation power in comparison with no additional impedance. Here, higher resonance frequencies lead to a reduction and above $f_{res} = 180\,GHz$ even to a suppression of the fluctuation power, which means that the bursting threshold current is increased above I_{above} by these added impedances.

THRESHOLD CURRENT & BURSTING FREQUENCY

For a more detailed investigation, a current scan has been simulated for two corrugation impedances. The ones chosen, are the impedance that produces the maximum intensity below and above the threshold ($f_{res} = 110\,GHz$) and the impedance with the lowest f_{res} to increase the threshold current above I_{above} ($f_{res} = 180\,GHz$). The Fourier transform of the emitted CSR power as a function of time is shown for a certain current range in the spectrograms in Fig. 3, in which the finger-like structure indicates the dynamics of

Table 1: Corrugation parameters for an additional impedance with the shunt impedance $Z_0=1\,k\Omega$ and the quality factor $Q = 3$

	$f_{res} = 110\,GHz$	$f_{res} = 180\,GHz$
corrugation depth h	$130\,\mu m$	$60\,\mu m$
periodic length L	$80\,\mu m$	$40\,\mu m$
corrugation width g	$40\,\mu m$	$20\,\mu m$
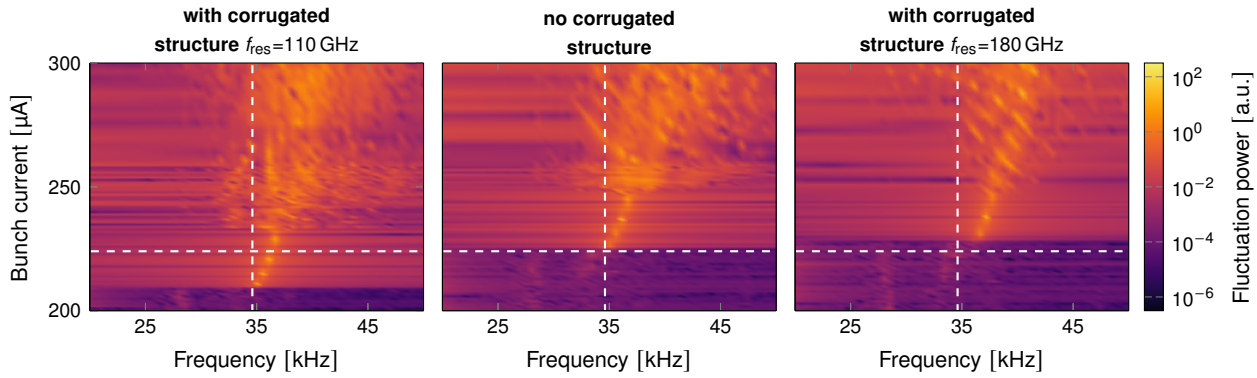
Figure 3: Color-coded power of the emission fluctuations for different bunch currents as a function of the fluctuation frequency around the bursting frequency f_{burst} without and with additional corrugation impedances for two resonance frequencies f_{res}. The shunt impedance and quality factor of the impedance were fixed at $Z_0 = 1\,\mathrm{k}\Omega$ and quality factor $Q = 3$, respectively. The horizontal white dashed line marks the start of the fluctuations due to the micro-bunching instability and the vertical one the corresponding bursting frequency for the case with no corrugated structure (middle).

the microbunching instability directly above the threshold current [11]. It can be seen, that the general shape of the finger and hence the bursting behavior of the microbunching is not substantially changed due to adding an impedance with $Z_0 = 1\,\mathrm{k}\Omega$. Nevertheless, the characteristic parameters of the bursting can be changed, notably the threshold current and the bursting frequency. In the spectrogram with the additional impedance of a corrugated structure with $f_{res} = 110\,\mathrm{GHz}$ it can be verified that the threshold current is reduced by $16\,\mu\mathrm{A}$ (7.1 %), whereas the bursting frequency of the fingertip stays unchanged.

In contrast, an additional impedance with $f_{res} = 180\,\mathrm{GHz}$ causes a slight increase of the bursting threshold by $3\,\mu\mathrm{A}$ (1.3 %). However, this additional impedance also increases the bursting frequency by about $1.9\,\mathrm{kHz}$, so that the longitudinal beam dynamics caused by the the instability are slightly modified. In Fig. 4 the threshold current and the bursting frequency at the fingertip are shown as a function

of the shunt impedance Z_0 of the additional corrugation impedance for the two different resonance frequencies considered in Fig. 3. It can be seen, that for each plot one of the parameters scales nearly linearly with the shunt impedance, whereas the respective other parameter does not significantly change.

SUMMARY & OUTLOOK

It is planned to install a corrugated structure into the KARA storage ring to study and manipulate the microbunching instability. Longitudinal beam dynamics and radiation emission simulations with the Vlasov-Fokker-Planck solver Inovesa showed that the resonance frequency of the additional impedance is the decisive parameter that determines how the instability is influenced, while the shunt impedance affects the intensity of the influence. By choosing the resonance frequency correctly, it is possible to either reduce the threshold current and therefore emit intense THz radiation at even lower bunch currents or to change the dominant fluctuation frequency of the microbunching.

As a next step, beam dynamics simulations with different machine settings will be carried out for understanding how the impedance affects the beam dynamics for different machine settings. Furthermore, we will design and fabricate the corrugated structures and the whole impedance manipulation chamber for the KARA storage ring.
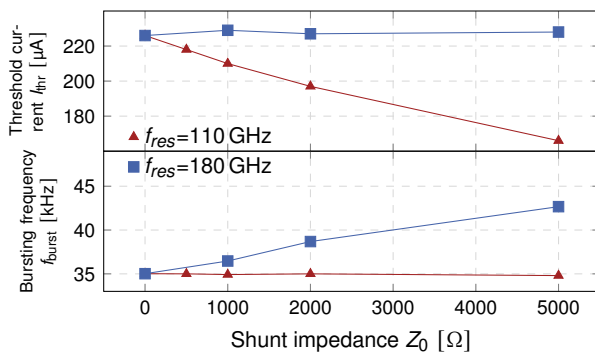
Figure 4: Bursting threshold and frequency for different shunt impedances Z_0. An additional impedance with a resonance frequency $f_{res} = 110\,\mathrm{GHz}$ (red) decreases the threshold current, whereas $f_{res} = 180\,\mathrm{GHz}$ (blue) increases the bursting frequency.

ACKNOWLEDGEMENTS

REFERENCES

[1] A.-S. Müller *et al.*, "Far Infrared Coherent Synchrotron Edge Radiation at ANKA", in *Proc. PAC'05*, Knoxville, TN, USA, May 2005, paper RPAE038, pp. 2518-2520.

[2] K. L. F. Bane, G. Stupakov, "Terahertz radiation from a pipe with small corrugations", *Nuclear Instruments and Methods in Physics Research A*, vol. 677, pp. 67-73, 2012.

[3] K. L. F. Bane *et al.*, "Measurement of terahertz radiation generated using a metallic, corrugated pipe", *Nuclear Instruments and Methods in Physics Research A*, vol. 844, pp. 121-128, 2017.

[4] K. Y. Ng *et al.*,"Explicit expressions of impedances and wake functions", Fermi National Accelerator Lab (FNAL), Batavia, IL (United States), 2010.

[5] CST Studio Suite, Dassault Systèmes, https://www.cst.com

[6] S. Maier, M. Brosi, A. Mochihashi, A.-S. Müller, M. J. Nasse, and M. Schwarz, "Impedance Studies of a Corrugated Pipe for KARA", in *Proc. IPAC'21*, Campinas, Brazil, May 2021, pp. 2039–2042. doi:10.18429/JACoW-IPAC2021-TUPAB251

[7] K. Y. Ng,"Impedances of bellow corrugations", Fermi National Accelerator Lab. (FNAL), Batavia, IL, USA, 1987.

[8] P. Schönfeldt *et al.*, *Inovesa*, 2017. doi:10.5821/zenodo.597356

[9] P. Schönfeldt *et al.*,"Parallelized Vlasov-Fokker-Planck solver for desktop personal computers", *Phys. Rev. Accel. Beams*, 2017. doi:10.1103/PhysRevAccelBeams.20.030704

[10] J. B. Murphy, R. L. Gluckstern, and S. Krinsky, "Longitudinal wakefield for an electron moving on a circular orbit", *Part. Accel.*, vol. 57, pp. 9-64, 1997. https://cds.cern.ch/record/1120287/

[11] M. Brosi *et al.*, "Fast Mapping of Terahertz Bursting Threshold and Characteristics at Synchrotron Light Sources", *Phys. Rev. Accel. Beams*, vol. 19, p. 110701, 2016. doi:10.1103/PhysRevAccelBeams.19.110701

[12] M. Brosi *et al.*, "Studies of the Micro-Bunching Instability in Multi-Bunch Operation at the ANKA Storage Ring", in *Proc. IPAC'17*, Copenhagen, Denmark, May 2017, pp. 3645–3648. doi:10.18429/JACoW-IPAC2017-THOBA1